

Relationship Between Steps in 8-Anilino-1-Naphthalene Sulfonate (ANS) Fluorescence and Changes in the Energized Membrane State and in Intracellular and Extracellular Adenosine 5'-Triphosphate (ATP) Levels Following Bacteriophage T5 Infection of *Escherichia coli*

V. Braun and E. Oldmixon

Mikrobiologie II, Institut Für Biologie II, Universität Tübingen, D-7400 Tübingen, Federal Republic of Germany

The addition of bacteriophage T5 to anaerobic, fermenting cells of *Escherichia coli* B or K-12 in the presence of 8-anilino-1-naphthalene sulfonate (ANS), N-phenyl-naphthyl-1-amine (NPN), or dansyl ethylamine causes the fluorescence of these probes to rise in two steps, the first occurring immediately upon addition, the second delayed by 6 min. The conditions necessary for observing this phenomenon are defined (cell density, probe concentration, substrate, absence of an electron acceptor, multiplicity of infection, growth, and harvesting conditions).

The magnitudes of the first and second steps in fluorescence are dependent upon the multiplicity of infection; the timing of the steps is not. The first step correlates with a breakdown in the potassium or rubidium permeability barrier of the cell, and it occurs either aerobically or anaerobically, with fermentable or nonfermentable substrates. The second step occurs only with cells that are without an available electron acceptor, are fermenting, and which have a functional membrane-bound, Ca^{2+} - Mg^{2+} -dependent adenosine triphosphatase (ATPase). The results are consistent with disturbance of energization of the cell membrane by the membrane-bound ATPase at the time of the second step in fluorescence. No change in the intracellular level of adenosine 5'-triphosphate (ATP) was seen, whereas the extracellular level increased sharply, starting 3–6 min after phage addition. The quantity of ATP found in the medium by 30 min after infection amounted to about four times the amount present inside the cells at the time of infection. The quantity and rate of efflux of ATP was similar under aerobic and anaerobic conditions.

Key words: ANS fluorescence, membrane hydration, cholesterol, phospholipid–cholesterol interaction, infrared spectra, red cell membranes

Received October 11, 1978; accepted December 5, 1978.

The bacterial virus (phage) T5 binds to an outer membrane receptor protein (for review see Braun and Hantke [1, 2] and Braun [3]). Binding triggers release of DNA from the phage head, which in turn is taken up into the cell by a two-step process. It is known that the second step requires cellular metabolism so that the cell actively participates in the infection. In the course of our studies on the translocation of the DNA biopolymer across the outer and the cytoplasmic membrane, we used fluorescence dyes as probes for membrane alterations. The fluorescence probe 8-anilino-1-naphthalenesulfonate (ANS) has been used to study changes in membrane energization in *Escherichia coli* cells [4]. ANS fluorescence increases when cell membranes are less energized, and it decreases when they are more energized [5]. Hantke and Braun [6] and Braun [7] have reported that ANS fluorescence in whole *E. coli* cells also increases following infection with phages T2 through T7. The fluorescence increase following phage T5 or BF23 infection can rise in two distinct steps [6], corresponding in time with DNA uptake in two steps in which first an initial 8% of the chromosome is transferred, then the remainder is transferred after several viral proteins (class 1 proteins) have been synthesized [8–10]. However, the transfer of the second DNA segment is not necessary for the second step of fluorescence to occur [6], indicating that the increase is probably due to the expression of functions directed by the first-step-transfer segment.

In this communication, we show that the nature of the phage-induced ANS fluorescence increase is similar to increases caused by a number of defects in energy metabolism; we also show that several features of the cell's response to phage infection are consistent with a phage-induced disturbance of the membrane-energizing activity of the membrane-bound, Ca^{2+} - Mg^{2+} -dependent adenosine triphosphatase (ATPase), which presumably leads to a dissipation of the transmembrane proton-motive force.

Inhibition of membrane energization by ATPase after T5 attachment to the cell is not due to a fall in intracellular ATP concentration. Although ATP begins to appear in the medium in large amounts following the sixth minute after phage addition, the amount of ATP within the cells remains constant. However, since excretion of ATP into the medium coincides in time with the second rise in fluorescence, the cell membrane presumably is seriously disturbed.

MATERIALS AND METHODS

Strains

The following bacterial strains were used (only relevant genetic markers are presented): *E. coli* B, *E. coli* F, *E. coli* K-12 Ymel, *E. coli* BH212 *uncA*, *E. coli* BH273 *uncA*, *E. coli* 26/4 *uncB*, *E. coli* 24/10 *uncB*, *E. coli* A1004C *hemA*. The last six strains were obtained from H. Schairer. The phage strains used were T5, T5⁺, T5stO, and BF23.

Fluorescence Probes

ANS (8-anilino-1-naphthalene sulfonate) and NPN (N-phenyl-naphthyl-amine) were obtained from Merck; dansyl EA, (5-dimethylamino-1-naphthalene sulfonyl ethylamine) was purchased from ICN Pharmaceuticals. ANS and dansyl EA were dissolved in 0.9% (w/v) NaCl in water, NPN in absolute ethanol. Excitation wavelengths were 313 and 366 nm, emission wavelengths 400–3,000 nm for ANS and NPN and 470–3,000 nm for dansyl EA.

Uncouplers and Inhibitors

Potassium cyanide (Merck, Darmstadt; analytical grade) was prepared in M9 buffer (see below, section on growth media used) at 100 mM immediately before use. *N,N'*-dicyclohexylcarbodiimide (DCCD) (Sigma Chemical Co.) was prepared as a 5 mM solution and stored at -20°C until use on the same day. 2-Trifluoromethyltetrachlorobenzimidazole (TTFB) (a gift from E. Bamberg, Konstanz) was prepared in absolute ethanol at a 1 mM solution and stored at 20°C until use. Ethanol concentrations in the samples did not influence the fluorescence or the cell behavior at the concentrations used (usually 1%).

Enzymes

Hexokinase (analytic quality) and glucose-6-phosphate dehydrogenase (G6PD, purity grade I) were obtained from Boehringer, Mannheim. Enzymes were supplied in 3.2 M ammonium sulfate solutions at pH 6.

Chemicals and Biochemicals

Nicotinamide adenine dinucleotide phosphate (oxidized form) (NADP) was obtained from Boehringer, Mannheim in the disodium salt form. Adenosine 5'-triphosphate (ATP) (crystallized disodium salt) was from the same source. All other chemicals were of analytical grade from Merck, Darmstadt, except for carbonylcyanide chlorophenylhydrazone (CCCP), a product of Sigma Chemical Co.

Radioactively Labeled Compounds

[2- ^3H]adenosine 5'-triphosphate, ammonium salt (^3H ATP) with a specific activity of 27 Ci/mmol was from Amersham-Searle, the Radiochemical Centre Ltd., Great Britain.

Cell Growth Conditions

The following minimal media were used: M9 [11]; a medium of Tanaka, Lerner, and Lin (TLL medium) [12]; and Cohen-Rickenberg medium (CR medium) [13], as modified by Anraku [14].

Cells induced for nitrate reductase were grown with shaking at 37°C in modified CR medium with 50 mM KNO_3 and 1 μM ammonium heptomolybdate [15] under H_2 - CO_2 atmosphere in a Gas-Pak[®] jar (trademark of Becton, Dickinson, and Co., Cockeysville, Maryland).

Growth and Purification of Bacteriophage T5

T5 bacteriophage were grown either on *E. coli* B, F, or K-12 Ymel on plates by the overlay technique. Phage were purified by sequential precipitation in polyethylene glycol 6000 (PEG) according to the method of Yamamoto et al [16]. The supernatant of a 2% PEG precipitation was given 6% additional PEG, kept at 4°C overnight, and then pelleted. The pellets were resuspended overnight in phage buffer (0.5 M NaCl, 1 mM CaCl_2 , 0.1 M Tris-HCl, pH 8.0, 0.01% gelatin) at 4°C and either used directly or purified further on CsCl step gradients according to Zweig and Cummings [17] or on density equilibrium CsCl gradients.

Fluorescence Experiments

Cells were grown in culture flasks filled to not more than 20% of their volume at 37°C in a rotary-motion water bath at about 200 rpm. Cell culture was measured in an

Eppendorf photometer (Model 1101M) at 578 nm. With a 1.0-cm light path, an absorbance of $A_{578} = 0.10$ is equivalent to 1.65×10^8 cells per milliliter under these growth conditions. The extinction was linearly related to the cell wet weight of the cultures through the range used for growth.

In a typical experiment, overnight cultures were inoculated from a single colony on a nutrient agar plate into a minimal medium with glucose (0.4%) as a carbon source. Cells from the overnight culture were then used to inoculate a new, experimental culture at about $A_{578} = 0.03$, and the culture was allowed to grow to an extinction between 0.10 and 0.14. Although the exponential growth phase continues beyond $A_{578} = 0.25$, cells taken from cultures with A_{578} greater than 0.14 often gave sluggish fluorescence responses. Cells were harvested by centrifugation. The clear supernatant was decanted, the tubes dried, and the cells gently and quickly resuspended in enough medium (no carbon source) to give a calculated final A_{578} of 1.0, that is, 1.65×10^9 cells per milliliter. In experiments with cells at a higher density, the pellet was resuspended to a calculated A_{578} of 10.0 (checked by reading the absorbance of a 1:100 dilution) and further diluted to the desired density in the cuvette.

Fluorescence was observed routinely with an Eppendorf photometer with fluorescence attachment and chart recorder. Cuvettes were quartz with an inner width of 7 mm and a path length of 5 mm. Cuvette temperature was maintained at 37°C by circulating water from a thermostated water bath through the jacketed cuvette holder. Recorder response was calibrated by adjusting the difference between the blue and green fluorescence standards (Eppendorf catalog No. 106501 and 106502 respectively; neutral-filtered sides used) to 25 scale divisions out of 100. The blue-to-green difference is our "arbitrary fluorescence unit." Using ANS at 60 μM under these conditions, the T5 infection of *E. coli* suspensions with $A_{578} = 1.0$ (to be described) gives a total response covering about two units, or half the chart width. Certain small, characteristic fluctuations associated with aerobic-anaerobic transitions in the cuvette were ascribable to NAD-NADH interconversions; spectra were taken with a Perkin-Elmer-Hitachi recording spectrofluorometer in Dr. Benno Hess's laboratory to establish this fact.

Exactly 1 ml of cell suspension was added to the cuvette, and the temperature was allowed to equilibrate. Then 10 μl of aqueous ANS solution was added (6 mM ANS, 0.9% NaCl). Sufficient 1-ml aliquots of ANS were kept frozen at -70°C for the entire series of experiments. The ANS was prewarmed to 37°C before addition to the cuvette, and the solutions were discarded at the end of the experiment. Carbon sources were added as 20 μl of 20% solutions, sterilized by filtration. Mixing of the sample was done either with a small, plastic paddle or by inverting the cuvette, covered with Parafilm several times.

Measurement of the ATP Content

The sensitivity of our method for ATP content determination is such that 20 A_{578} absorbance units of cells (that is, about 3.3×10^{10} cells) give a definite, reproducible reading. Therefore, for an experiment with eight samples from a suspension at $A_{578} = 5.0$, 32.2 ml of cell suspension was added to each flask. (The 0.2 ml extra provided a safety margin.) The contents of the flasks were continually bubbled at 37°C with water-saturated air or argon. After 10 or 15 min, glucose was added to 20 mM, and the incubation was continued for no longer than 10 min. (The pH of such thick cell suspensions starts to fall even in a buffered medium like M9 as soon as a fermentable carbon source is present.) During this preincubation time, the fluorescence responses of the cells were checked to be sure that they were typical with regard to speed and magnitude of response to aeration,

addition of glucose, and phage addition. The fluorescence of a pilot sample was also followed throughout the sampling experiment. The cultures were thoroughly agitated during and shortly after phage addition. Samples were removed at the times indicated, each sample containing $20 A_{578}$ units of cells; they were pipetted directly over pulverized, frozen M9 medium (no glucose) and were spun for 10 sec at 15,000 rpm at 0°C . The entire process from sampling to firm cell pellet and decanted supernatant took less than 120 sec, less time than required to separate this quantity of cells from medium by filtration methods.

The supernatant was decanted and stored in ice. Then 1 ml of 5% (w/v) perchloric acid was added to the cell pellet, which was vortexed vigorously for 60 sec and stored on ice until the end of the sampling. The pellets, which became noticeably more difficult to resuspend at later sampling times, were additionally dispersed in the perchloric acid with ultrasound (1 sec, repeated three times). The resuspended pellets were further incubated 10 min at 0°C ; then the denatured protein was spun down. From each supernatant 1 ml was carefully removed and cautiously neutralized to pH 6.8–7.0 using 6 N K_2CO_3 0.5 M triethanolamine (TRA, pH 7.4), with continuous mixing during addition. The pH was not allowed to exceed 7.0. The precipitated KClO_4 was removed from the neutralized sample by holding on ice for at least 10 min, then centrifugation; 800 μl of the supernatant was carefully pipetted off and stored at 4°C until testing.

The original cell supernatants were each filtered through presoaked (in 0.1 M LiCl aqueous solution) cellulose acetate filters (Millipore Corp., 0.45- μm pore size) to remove any remaining cells. The filtrates were stored at 4°C until testing.

ATP Assay

The procedure followed is based on that of Estabrook et al [18]; its successful use in an E coli system has been reported [19]. To assay the pellet extract (intracellular ATP), the contents of a cuvette were assembled in the following order: 740 μl partial reaction mix (PRM; 50 mM TRA, pH 7.4, 10 mM KCl, 10 mM MgCl_2 , 5 mM EDTA, pH 7.4), 200 μl sample, 10 μl 1 M glucose, and 10 μl 1 mM NADP. The chart zero was adjusted, then 20 μl hexokinase (1 $\mu\text{g}/\text{ml}$) was added. The baseline was established, then 20 μl G6PD (2 $\mu\text{g}/\text{ml}$) was added. (This order of addition of the enzymes is reversed from that recommended by Estabrook [18], but we have obtained better, more consistent results with this procedure. The error due to the possible presence of G6PD is insignificant in this system.)

To assay the medium for extracellular ATP, the cuvette contents were made up as above, except that 440 μl PRM and 500 μl sample were used. The amount of ATP in a sample was determined by recording the fluorescence increase for 4 min. The fluorescence curve given by a reagent blank (no ATP; appropriate buffer only) was subtracted from this curve, and the resulting values at 2, 3, and 4 min were averaged. This value was compared to a standard curve of the range 0–5 nmoles ATP per cuvette prepared separately for each sample type for each experiment, using a fresh ATP solution whose ATP concentration was checked spectrophotometrically (molar extinction coefficient of ATP at 259 nm = 1.540×10^4 ; source: Mathis and Brown [20]). The standard curves prepared by this method are linear between 0 and 4 nmoles ATP per cuvette. The amount of ATP in the cuvette was then corrected back to the ATP concentration in the original sample, as molecules ATP/cell, using the following expressions:

$$\frac{\text{molecules ATP}}{\text{cell}} = \frac{\Delta\text{FL} \cdot V \cdot 6.023 \cdot 10^{14}}{\text{SAC} \cdot \text{sn}}$$

where ΔFL is the observed fluorescence increase in arbitrary units; S , the volume removed from the cell suspension as sample (in milliliters); s , the volume of extract or filtered medium added to the cuvette (in milliliters); V , the volume of extracts after neutralization (in milliliters); A , the optical density of sampled cell suspension; n , the number of cells per optical density unit per milliliter (equals 1.65×10^9 under our conditions); C , the slope of the standard curve, as $\Delta FL/n\text{moles ATP}$ in cuvette.

ATP Uptake Into Anaerobic, Fermenting Cells

Cells were prepared as described above. Gastight syringes (5 ml) with 50-step repetitive dispensing devices (Hamilton Co., Reno, Nevada) held at 37°C were filled with the proper amount of phage with $5 \mu\text{Ci}$ [^3H] ATP (1 fM ATP, final concentration in cell suspension) in a total volume of 0.2 ml (brought to this volume with M9 medium). Samples of cells (0.2 ml) at 37°C in M9 medium with glucose at $A_{578} = 5.21$ were dispensed onto presoaked (in 0.1 M LiCl) cellulose acetate filters under suction (40 cm Hg) and washed with 3 ml 0.1 M LiCl. The retained radioactivity was measured in a scintillation counter.

RESULTS

Fluorescence Changes Caused by Phage T5 Infection

Attention had been drawn to this system by the observation [6, 7] that the infection of *E. coli B* by T5 in the presence of ANS prompted the probe fluorescence to rise in two stages, one occurring immediately, another delayed by about 6 min (Fig. 1). The features of the curves in Fig. 1 will be presented in more detail later in the text. The following remarks apply equally to all of the wild-type T5 and to the very similar phage BF 23. The experiments may be performed with *E. coli B* or with the K-12 strains listed. *E. coli F*, although used to produce the T5 phage, shows an erratic fluorescence response upon T5 infection and has not been used in these experiments.

The sizes of the individual steps in the fluorescence rise were related to the average number of phage infecting per cell, that is to the multiplicity of infection (MOI). The curves in Fig. 2 show that between MOIs of about 0.6–6 there was a fluorescence increase between the preinfection level and the level 5 min after infection (step 1) and also a proportionality between the fluorescence increase from 5 minutes to 12 minutes after infection (step 2) and the MOI.

Although the sizes of the steps were influenced by the number of infecting phages per cell, the shapes and timing of the two steps were not affected in this range of MOIs. Figure 3 shows the enveloped of normalized curves resulting from infections at MOIs from 0.6–6 and the average of the curves within this envelope. The shapes of the normalized curves are very similar. Figure 4 shows a more sensitive test of the effect of increasing MOI on the fluorescence response. By taking the first derivatives of the envelope boundaries of the normalized curves and of the averaged curve, it was shown that the timing of the curves varied by less than a minute. Thus, increasing the MOI only expands the fluorescence curve vertically; shifting along the time axis appears to be negligible.

The ANS fluorescence curves obtained after T5 infection are influenced by a number of factors, among them the cell density in the cuvette, the ANS concentration, and the MOI. To clarify the effect of each of these factors, we systematically varied separately each of these quantities. The results of this search are shown in Fig. 5. The effect of increasing the ANS concentration from 60 to 180 μM shows the expected magnification of response, but no change in the pattern of the response when this factor alone is varied. Increase of the number of phages per cell (MOIs of 3 to 9) results in a

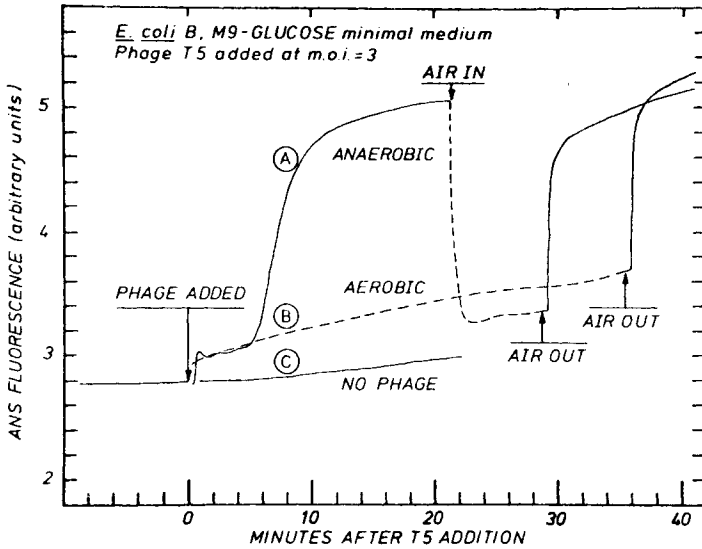


Fig. 1. Effect of T5 phage infection on aerated and unaerated E coli B on ANS fluorescence. Cells of E coli B were incubated at 1.65×10^9 cells per milliliter in M9 medium containing 0.4% glucose and $60 \mu\text{M}$ ANS. Curve A shows cells incubated anaerobically during the time prior to phage addition at MOI = 3.0 at time 0 (indicated by "Phage added"), then aerobically for about half a minute after phage addition, returning to anaerobic conditions. Air was bubbled into the cuvette 22–29 min after phage addition. Curve B shows cells aerated before and after phage addition; air was shut off at 36 min after phage addition. Curve C shows cells incubated anaerobically throughout and not infected with phage. Solid lines after time 0 indicate no aeration, and dashed lines mark bubbling.

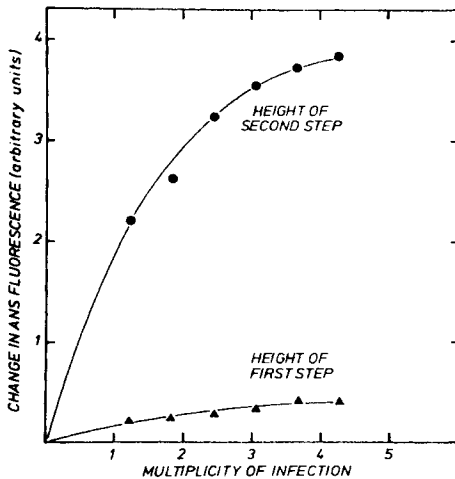


Fig. 2. Effect of multiplicity of infection on the magnitudes of the first and second steps in ANS fluorescence. Cells were incubated as described in Materials and Methods and in legend to Fig. 1. The height of the first step is the change in ANS fluorescence from 1 min before phage addition to 5 min after; the height of the second step is the change from 5 min to 12 min after infection.

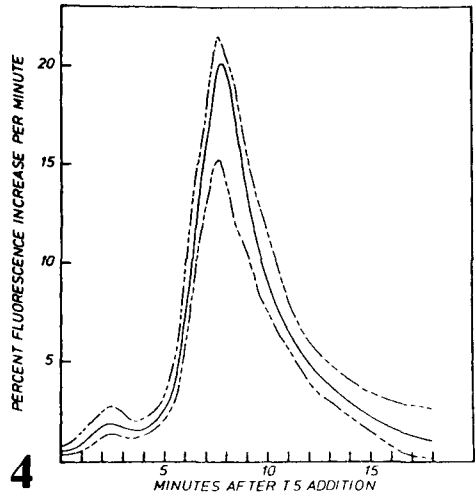
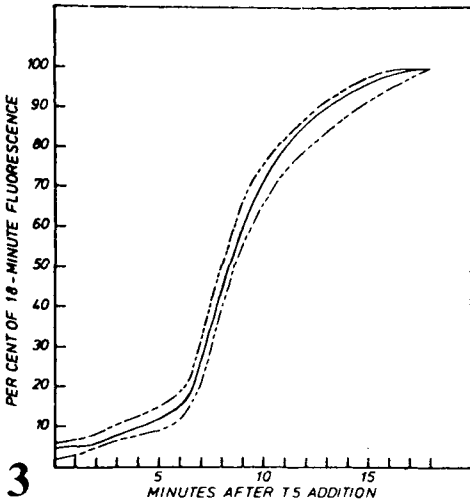


Fig. 3. Composite curve of ANS fluorescence responses of E coli B infected at various MOIs. The curves supplying the data for Fig. 2 were normalized to give 100% fluorescence change by 18 min after infection. The solid curve marks the average; the dotted lines mark the farthest outlying values of the contributing curves.

Fig. 4. Rate of ANS fluorescence increase in the two-step curve after T5 addition at various MOIs, plotted against time after phage addition. Curve was computed from the normalized data used in Fig. 3 for each separate MOI curve. The average rate of change of fluorescence is shown by the solid line, and the envelope of farthest outlying values is indicated by the dashed lines.

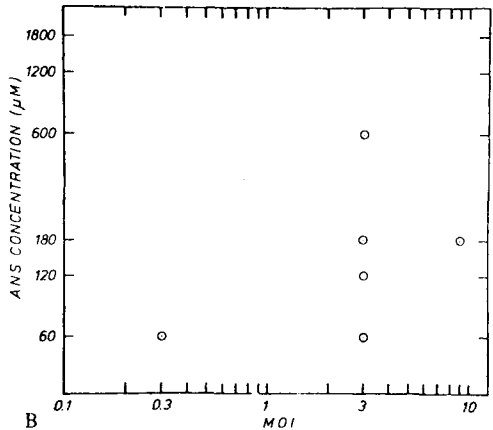
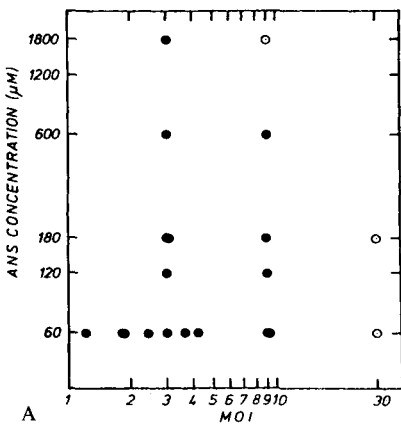


Fig. 5. Conditions required for observing a two-step rise in ANS fluorescence after T5 phage addition: cell density, ANS concentration, MOI. A: Washed E coli B resuspended in M9 medium, with 0.4% glucose as carbon source, at 1.65×10^9 cells per milliliter. The observed part of the cuvette is anaerobic under these conditions. Phage T5st0 added at the multiplicities shown, with ANS present at the concentrations indicated. ●) A two-step curve was seen; ○) a single, immediate rise to a high fluorescence was seen. B: Conditions the same as in A, except that the cells were resuspended at $A_{578} = 10.0$, or 1.65×10^{10} cells per milliliter. At this cell density a single, large fluorescence rise was seen, regardless of MOI or ANS concentration used. Intermediate cell densities, between 1.65×10^9 and 1.65×10^{10} , gave results described in the text.

larger response at the higher MOIs but not a change of type. The cell density, however, had a distinct effect on the response pattern. The immediate change in fluorescence (what we have called the first step) became larger, and larger, finally almost entirely swamping the second step at $A_{578} = 8$. At higher cell densities one sees only an immediate rise in ANS fluorescence that continues, at a reduced but constant rate, for over 20 min. This high fluorescence is not reversible by aeration, which suggests that at this stage the membrane cannot be significantly reenergized by the electron transport chain (ETC), or that if it does occur, ANS no longer indicates it.

Fluorescence Change and Membrane Energization

ANS fluorescence apparently bears a relationship to the energization of the bacterial cell membrane [5, 21–23], and our observations support this view, with modifications. Washed cells held anaerobically without an energy source responded with a sharp increase in fluorescence comparable in size to step 2 seen after T5 infection. If we consider that the membrane may be energized either through the action of the electron transport chain or coupled with ATP hydrolysis by the membrane-bound, Mg^{2+} - Ca^{2+} -dependent ATPase, then the following conditions should energize the membrane and reduce the ANS fluorescence: 1) provision of oxygen, allowing energization by way of the ETC (Fig. 6A); 2) provision of an alternate electron acceptor, such as nitrate, to appropriately induced cells, allowing energization by the ETC (Fig. 6B); 3) provision of a fermentable substrate such as glucose to cells with a functional membrane-bound, Mg^{2+} - Ca^{2+} -dependent ATPase, whereby ATP generated by glycolysis would be hydrolyzed by the ATPase and proton gradient generated, which is equivalent to membrane energization (Fig. 6C).

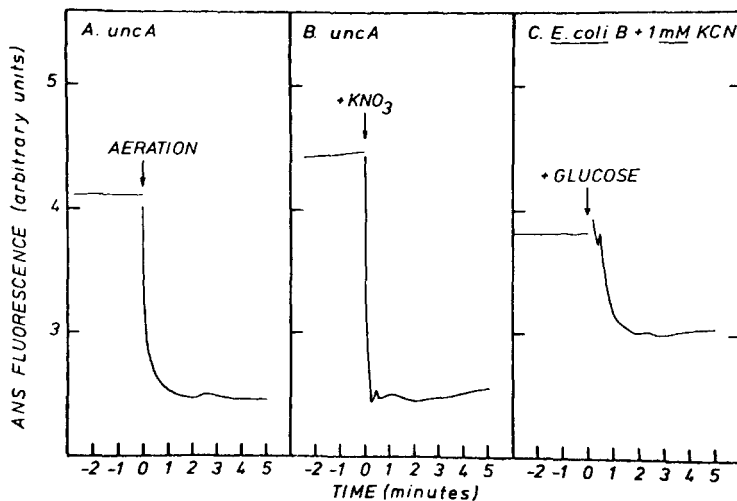


Fig. 6. Conditions allowing ongoing membrane energization, as shown by decreased ANS fluorescence. Cell sample preparation as described in the text and in legend to Fig. 1. A: *E. coli* K-12 BH212 *uncA* mutant (lacking ATP hydrolyzing activity in the F_1 portion of the membrane-bound, Mg^{2+} - Ca^{2+} -dependent ATPase) was induced for nitrate reductase and held anaerobically in the cuvette, producing the level part of the curve to the left. Air was introduced by bubbling, and the fluorescence dropped to a lower intensity, indicating energization via the ETC, using oxygen as the electron acceptor. B: Argon-flushed KNO_3 (50 mM final concentration) was added to a sample identical to that in A. The fluorescence dropped immediately and remained low for the rest of the experiment. That indicates energization by the ETC, using nitrate as the electron acceptor in the absence of oxygen. C: *E. coli B* was poisoned with 1 mM KCN so as to show no fluorescence decrease when aerated; the cells were resuspended without glucose. When glucose was added to 0.4% final concentration, the ANS fluorescence was reduced, presumably indicating membrane energization by hydrolysis of ATP produced through glycolysis.

In contrast, the following conditions would not establish a proton-motive potential, an increase in membrane energization, or a lasting decrease in ANS fluorescence from the high, step 2 level: 4) aeration of cells lacking a functional ETC, such as a hemA mutant grown without δ -aminolaevulinic acid, or nonfermenting cells poisoned with 1 mM cyanide (Fig. 7, left); 5) provision of an alternate electron acceptor to cells uninduced for the appropriate enzymatic oxidation-reduction system; 6) addition of a nonfermentable substrate such as succinate to cells with a functional (but not functioning) membrane-bound, Mg^{2+} - Ca^{2+} -dependent ATPase, held anaerobically; or 7) provision of a fermentable substrate, anaerobically, to cells lacking a functional ATPase (uncA or uncB mutants) (Fig. 8, left).

In fact, each of these seven predictions was fulfilled, in experiments with a variety of wild-type and mutant strains and a range of fermentable and nonfermentable substrates, and with ANS as the fluorescence probe. Not all of these conditions were tested using NPN or dansyl EA but, where tested, no aberrations were observed. Therefore, ANS, NPN, and dansyl EA seemed to indicate, by decreased fluorescence with whole cells, conditions under which a proton-motive potential across the bacterial membrane was being actively established and maintained.

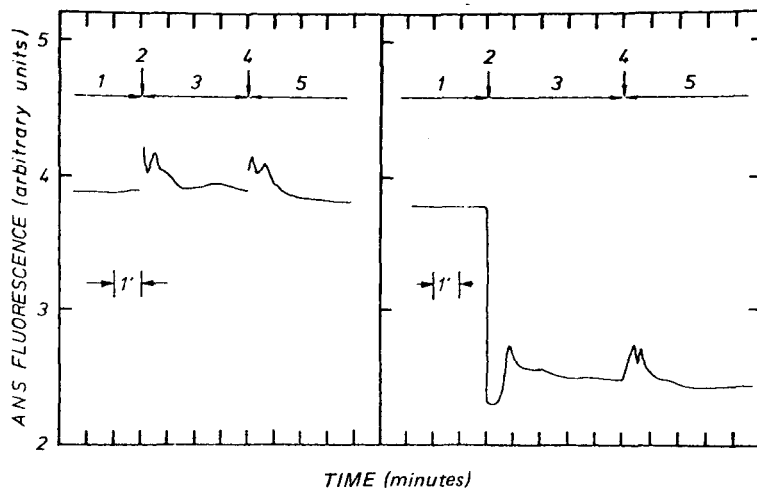


Fig. 7. Left: Washed *E. coli* K-12 BH212 *uncA* cells were resuspended in M9 medium to a cell density of 1.65×10^9 cells per milliliter with $60 \mu M$ ANS, 1 mM KCN, and no carbon source. The cells are anaerobic under these conditions, cannot energize the membrane, and have a high fluorescence, as seen in section 1 of the curve. At the time indicated by arrow 2, the cells were given succinate to 0.4% final concentration and aerated briefly. They were unable to utilize the oxygen and the nonfermentable substrate to energize the membrane and reduce the ANS fluorescence, as seen in section 3 of the curve. At arrow 4, the cells were given glucose to 0.4% final concentration, and were pulse-aerated. Here also they are unable to energize the membrane, in this case because of the mutation disabling the membrane-bound ATPase, as seen in section 5 of the curve. Right: Washed *E. coli* B cells were resuspended in M9 medium to cell density of 1.65×10^9 cells per milliliter, without a carbon source, with ANS at $60 \mu M$, giving the high fluorescence shown in section 1 of the curve. Glucose was added to 0.4% final concentration, and the cells were pulse-aerated at arrow 2. The fluorescence dropped at once to the lower level characteristic of aerated cells, underwent the aerobic-anaerobic transition, and remained at the level characteristic of cells energizing their membrane by fermentation, as seen in section 3. At arrow 4, KCN was added to 1 mM final concentration, and the cells were pulse-aerated. As seen in section 5, the cells remained at the low, fermenting level, even though the ETC had been incapacitated.

Various agents are available that disturb the ETC, block the membrane-bound ATPase, or provide relatively unrestricted passage across the membrane to protons, thus breaking down the proton-motive potential. Potassium cyanide, for example, falls in the first class, DCCD in the second, and TTFB and CCCP in the third.

Agents acting directly against the ETC (potassium cyanide, for example) [24, 25] would not be expected to dissipate a proton-motive potential due to the action of the ATPase and therefore would not cause ANS fluorescence to increase. Potassium cyanide added at 1 mM final concentration gave results that agree with the predictions above. When potassium cyanide (1 mM final concentration) was added to cells energized only through the ETC, ANS fluorescence rose (Fig. 9, left). When added to cells energized by hydrolysis of ATP generated by glycolysis, though, cyanide did not cause a fluorescence increase (Fig. 7, right).

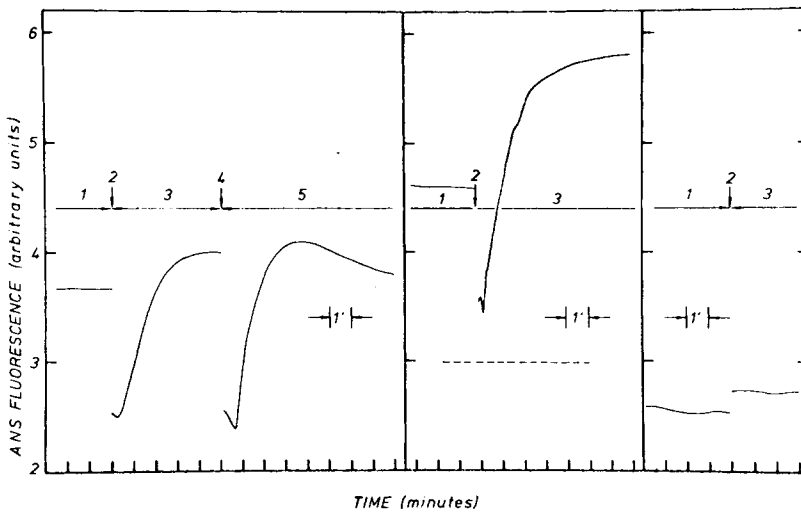


Fig. 8. Left: Cells of E coli K-12 BH212 *uncA* were resuspended to a cell density of 1.65×10^9 cells per milliliter, in M9 medium, without carbon source, with $60 \mu\text{M}$ ANS. The cells were anaerobic, with a high fluorescence in section 1 of the curve. At arrow 2, succinate was added to 0.4% final concentration, and the cells were pulse-aerated. Section 3 of the curve shows that the cells energized their membrane using the available oxygen but that the energization faltered, that is, the ANS fluorescence rose as the conditions became anaerobic. With a nonfermentable substrate, the cells could not maintain an energized membrane state. At arrow 4, glucose was added to 0.4% final concentration, and the cells were pulse-aerated. In section 5 of the curve, the air was used for energization and was exhausted, and the membrane was no longer being actively energized, as seen by the rising fluorescence. These cells could not use glucose for membrane energization, since their membrane-bound ATPase was defective. Middle: E coli K-12 BH212 *uncA* cells were resuspended as above, with 0.4% glucose as carbon source. Cells that are continuously aerated give a fluorescence at the level of the dashed line; unaerated cells have a fluorescence at the level shown by section 1 of the curve. At arrow 2, DCCD was added to a final concentration of $100 \mu\text{M}$ and was pulse-aerated. Section 3 of the curve shows initial drop in fluorescence in response to aeration, and then a return to high fluorescence as conditions become anaerobic. The overshoot in fluorescence above the previous level is an effect observed at this concentration of DCCD; we find that the additional rise, which is not reversible by aeration, is smaller at lower concentrations. Right: Cells of E coli K-12 BH212 *uncA* were resuspended as above, but constantly aerated throughout. DCCD was added at a final concentration of $100 \mu\text{M}$ at arrow 2. Section 3 of the curve shows that DCCD did not cause a major change in the fluorescence of aerated cells.

DCCD also caused the expected changes in ANS fluorescence. If anaerobic cells were actively fermenting, the addition of DCCD to a final concentration of $100\ \mu\text{M}$ was followed promptly by a large, step 2-like fluorescence increase. The results shown in Figure 9, right, are consistent with the assumption that DCCD blocks the proton channel in the ATPase's membrane-contained (F_o) portion [26–28]. Since DCCD should not interfere with the pumping of protons by the ETC, aeration should lower the ANS fluorescence, and in fact DCCD had little effect on the fluorescence of aerated *uncA* or *uncB* cells (Fig. 8, right). If *uncA* or *uncB* cells with an inactive ETC and resultant high ANS fluorescence were to be given DCCD, one would not expect the degree of energization of the membrane or the ANS fluorescence to be influenced; the ATPase would be inactive to start with, owing to the mutations. Figure 8 (center) shows the effect of DCCD on unaerated *uncA* cells. An additional steady fluorescence rise occurs, but the amount of aeration-reversible fluorescence increase remains relatively constant after DCCD addition.

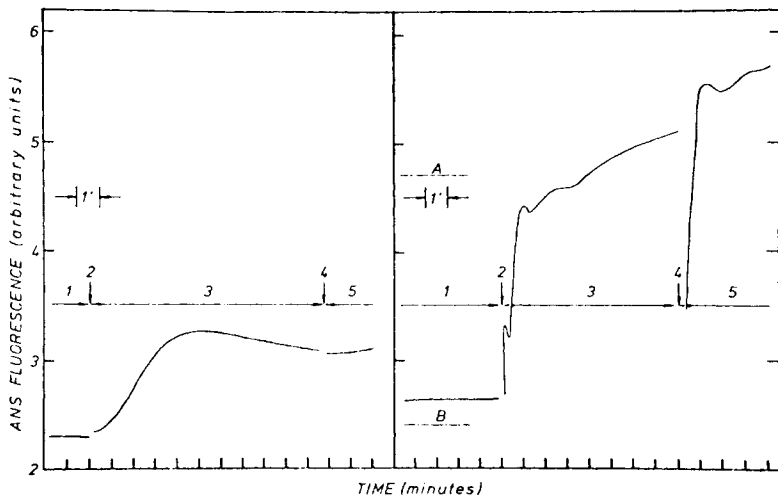


Fig. 9. Left *E. coli* K-12 BH212 *uncA* cells were resuspended in M9 medium at a cell density of 1.65×10^9 cells per milliliter, with 0.4% glucose, and $60\ \mu\text{M}$ ANS. Section 1 of the curve shows fluorescence obtained when cells were aerated continuously. At arrow 2, KCN was added to $100\ \mu\text{M}$ final concentration. Section 3 of curve shows that fluorescence rose, owing to inactivation of the ETC. At arrow 4, aeration was stopped. Section 5 of curve shows that no additional rise in fluorescence occurred, indicating that the cyanide had achieved its maximal effect on the fluorescence. As seen in Fig. 7, left, the addition of cyanide at $1\ \text{mM}$ final concentration had no effect on the fluorescence of unaerated cells under otherwise identical conditions. Right: *E. coli* B cells were resuspended to a cell density of 1.65×10^9 cells per milliliter in M9 medium, with 0.4% glucose as carbon source and $60\ \mu\text{M}$ ANS. The dashed line A indicates the level of fluorescence given by unaerated cells before the addition of glucose. Dashed line B shows the level of fluorescence given by cells with glucose and with continuous aeration. Section 1 of the curve shows the fluorescence associated with unaerated cells in the presence of 0.4% glucose. At arrow 2, DCCD was added to a final concentration of $100\ \mu\text{M}$, and the cells were pulse-aerated. Section 3 of the curve shows that the fluorescence rose sharply to about the level of dashed line A, associated with cells not actively fermenting or energizing the membrane through the action of the ATPase. The cells were aerated shortly at arrow 4 to establish that the fluorescence rise caused by DCCD was largely reversible by aeration, i.e., the action of the ETC. The background effect, which is not reversible by aeration, is evident here.

Representatives of the third class of substances, the true "uncouplers," such as TTFB or CCCP, drastically increase the cell membrane's permeability to protons. These agents, therefore, should be able to deenergize a membrane whether the proton-motive potential is generated by the ETC or the ATPase. ANS fluorescence increased after TTFB was added to the cells at a final concentration of $10 \mu\text{M}$ (Fig. 10). The fluorescence increase could be reversed by aeration, but more vigorous bubbling was required than to reverse, for instance, the DCCD-induced fluorescence. The addition of T5 phage to cells treated with TTFB or CCCP had essentially no additional effect on the fluorescence. These observations are also consistent with the view that a decrease in ANS fluorescence signals membrane energization by the ETC, the ATPase, or both, and that increasing ANS fluorescence indicates a breakdown in this energized state.

Relationship Between Energy-Dependent and T5-Dependent Fluorescence Change

The relationship between the two-step fluorescence increases following T5 infection and the energized membrane state was investigated using these observations as guides. The following questions were asked:

1. Are there parallels between the T5 step 2 and increases seen under other conditions?
2. If step 2 does apparently signal the dissipation of the energized state, is this caused by action specifically against the ETC's function, specifically against the action of the ATPase, or is it a nonspecific, generalized destruction of the proton-motive potential?

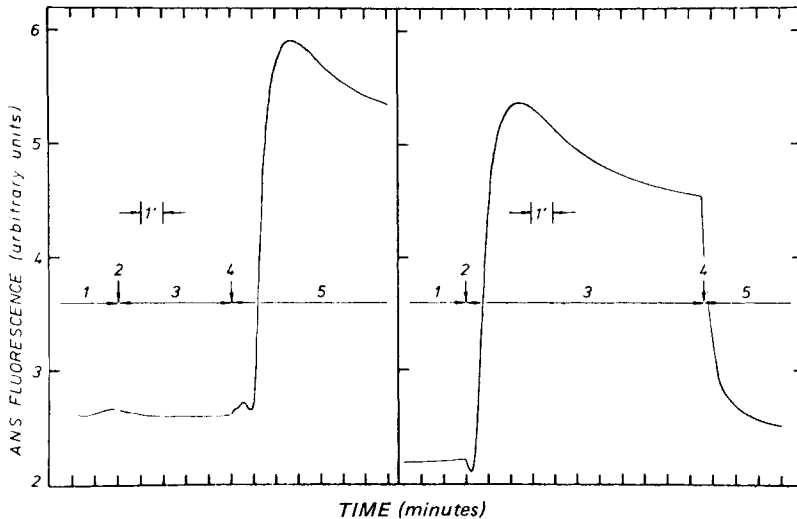


Fig. 10. Left: *E. coli* B cells were resuspended at a cell density of 1.65×10^9 cells per milliliter in M9 medium, with 0.4% glucose and $60 \mu\text{M}$ ANS. Section 1 of the curve shows the fluorescence of continuously aerated cells. At arrow 2, TTFB was added to $10 \mu\text{M}$ final concentration, and aeration was continued. Section 3 of the curve shows that the energization of the membrane via the ETC was strong enough to counteract the uncoupling effect of TTFB. At arrow 4, the aeration was discontinued, and the fluorescence rose immediately, with an overshoot, as seen in section 5. Right: The same conditions as in the left portion of the figure, except that the cells were not aerated in section 3 of the curve, after the addition of TTFB, showing the immediate effect of this uncoupler. At arrow 4, aeration was recommenced, resulting in the low fluorescence seen in section 5 of the curve. Strong aeration was necessary to drive the fluorescence down. Intermediate rates of aeration would have shown intermediate levels of fluorescence.

The first question may be answered provisionally by remarking that *uncA* and *uncB* mutants undergoing an aerobic-anaerobic transition showed a step 2-like increase that had approximately the same magnitude as the T5 step 2, both of which were reversible by ETC action. The fluorescence increase accompanying an aerobic-anaerobic transition with wild-type cells with a fermentable substrate but with added DCCD also mimics the T5 step 2. Also, cells with a nonfermentable substrate, such as succinate, show this kind of fluorescence increase as they go anaerobic. Consequently, the similarities seem to lie with those conditions that disturb membrane energization by ATPase, whether caused by the type of substrate offered to the cells, internal modifications due to mutation, or externally added chemicals, or by addition of the phages T5 or BF23.

The answers to the second question reinforce this tentative conclusion. Conditions were arranged so that cells were able to energize the membrane only through the activity of the ETC, even though intracellular ATP was present; aerated *uncA* or *uncB* cells in the presence of a fermentable substrate were used for this system. Infection by T5 did not cause a rise in fluorescence after 6–10 min. The experiment was repeated using cells lacking a functional ATPase but induced for nitrate reductase. When held without oxygen but given nitrate as an alternate electron acceptor, T5 infection did not cause a step 2-like fluorescence (Fig. 11). The T5 phage evidently did not disrupt the activity of the ETC.

Cells can be set up with an actively working ATPase and an inactive ETC; wild-type cells held anaerobically in the presence of glucose fit this description. When infected with T5, such cells showed the two-step fluorescence curve (Fig. 1), and these are the conditions under which the original observations [6] were made.

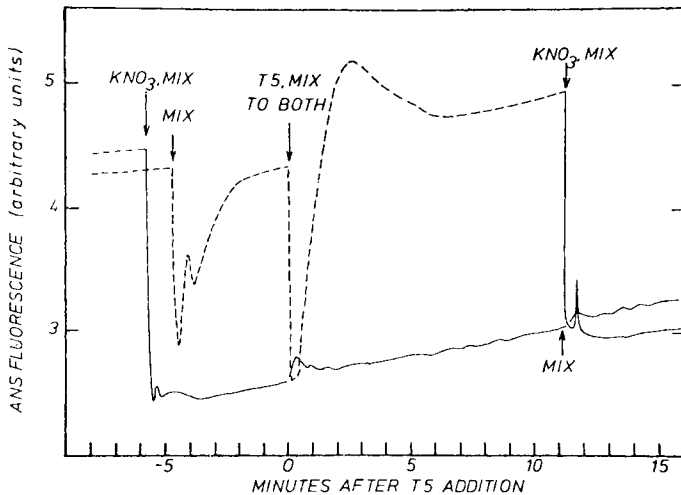


Fig. 11. Demonstration that T5 infection does not interfere nonspecifically with membrane energization processes or specifically with energization via the ETC. *E. coli* K-12 BH212 *uncA* cells were induced for nitrate reductase as described in Materials and Methods. The dashed line indicates a cell sample without KNO_3 ; the solid line indicates one with KNO_3 . The lower curve shows the fluorescence of cells with KNO_3 added at -4 min, as indicated. Fluorescence dropped immediately and remained low throughout the course of the experiment, even after T5 addition at $\text{MOI} = 3$ at 0 time. The upper curve shows a sample to which air was introduced in order to establish the response to aeration during the introduction of KNO_3 . The stronger, constant effect of the nitrate is clear. Phage were added to $\text{MOI} = 3$ at 0 time. After an overshoot, the fluorescence returned to a level slightly above the extended line of the fluorescence before phage addition. Subsequent addition of KNO_3 to this sample caused the fluorescence to drop, indicating that the ETC was still functional after phage addition.

T 5 Infection Leads to ATP Excretion

Having defined lack of membrane energization via ATPase as the most likely cause of the second fluorescence rise upon T5 infection, we determined whether the cells run out of ATP.

Figure 12 shows the amounts of ATP found intracellularly and extracellularly, under anaerobic and aerobic conditions, when cells at $A_{578} = 5$ are infected at an MOI of 5. The difference between the levels of extracellular ATP seen in infected and uninfected samples is massive. On the other hand, the difference between the ATP levels seen in the anaerobic and aerobic samples is small and probably not significant. In this figure, the extracellular ATP level seems to increase constantly from the time of infection, but this is due to the timing of the samples. More frequent sampling revealed that the rate of ATP appearance in the medium was slower from 0 to 6 min after infection than from 6 to 9 min, paralleling the ANS-E coli fluorescence curves (Fig. 13). The amount of ATP excreted increased with rising MOIs (in Fig. 13 shown only for anaerobic conditions) similar to the increase in ANS fluorescence.

If ATP appears in the medium because the cell membrane becomes leaky and permeable to ATP, then ATP added to the medium should be able to pass into the cell and be measured there. Figure 14 shows the results of an experiment in which [³H] ATP and various amounts of T5 phage were added to an anaerobic cell suspension ($A_{578} = 5.0$), with samples removed, filtered, and washed every 30 seconds, as described in Materials and Methods. Clearly, the amount of nonfilterable, labeled material rises with increasing time after infection, especially at the lower MOIs. The fact that increasing the MOI lowers the

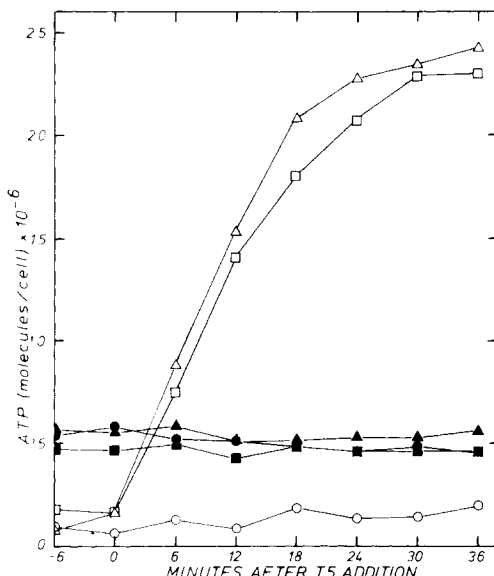


Fig. 12. Intracellular and extracellular ATP levels under aerobic and anaerobic conditions after T5 infection of E coli cells. Cells prepared as described in Materials and Methods. Three pairs of ATP levels are shown here; intracellular levels by filled symbols, extracellular levels by empty symbols. Symbols: ●, ○ control results (no phage added) under aerobic conditions; ▲, △ MOI = 5, aerobic; ■, □ MOI = 5, anaerobic.

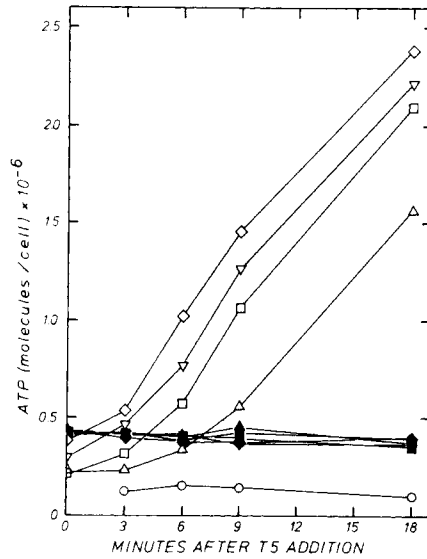


Fig. 13. Intracellular and extracellular ATP levels after T5 infection of *E. coli* under anaerobic conditions: sampling more frequent than in Fig. 12. Conditions as above; filled symbols indicate intracellular ATP levels, empty symbols show the extracellular levels, Symbols: ●, ○) MOI = 0; ▲, △) MOI = 1; ■, □) MOI = 3; ▽, ▾) MOI = 5; ◆, ◇) MOI = 7.

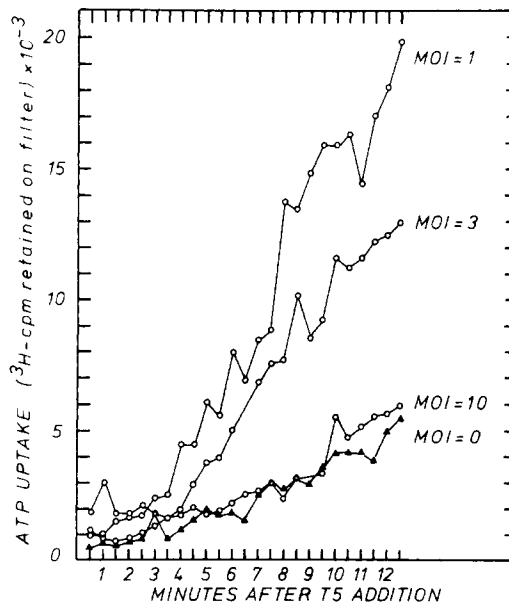


Fig. 14. Retention of externally added [^3H]ATP by *E. coli* cells after T5 phage addition. Experimental conditions described in Materials and Methods; cells of *E. coli* B at $A_{578} = 5.0$ under anaerobic conditions in M9-glucose medium. T5 phage added at zero-time at the MOIs shown.

amount of label retained on the filters (and, presumably, the amount of [³H]ATP taken up by the cells) is probably due to the greater amounts of ATP released into the medium at the higher MOIs, thus diluting the labeled ATP with “cold, carrier” ATP from the cells themselves. That this could occur was shown by experiments in which a starting, external ATP concentration of 5 mM unlabeled ATP and 1 fM [³H]ATP resulted in essentially no uptake of the label (results not shown).

Providing 5 mM ATP externally to the cells at various times before or after infection did not prevent or reverse the two-step fluorescence change (anaerobic cells at $A_{578} = 5$ in M9-glucose medium, infected at MOI = 3).

DISCUSSION

Starting from the initial observation of Hantke and Braun [6] that infection of *E. coli* with T5 phage could result in a two-step increase in ANS fluorescence, we began by defining the range of conditions under which this response could be observed and by surveying the effects of various treatments and mutations to see which would cause a similar fluorescence increase. Having defined the conditions under which the two-step increase occurs, we examined the components of the response to see how much change would be aeration-reversible, and whether the timing and size would change with increasing MOI. The first, immediate rise in fluorescence most likely indicates a breakdown in the membrane permeability barrier to small ions as revealed by rubidium ion efflux [29]. Our results concerning the second fluorescence increase led us to the working hypothesis that T5 phage infection does not affect directly the activity of the electron transport chain, but rather that it counteracts the energization of the membrane by the membrane-bound ATPase.

This supposed inability could be due to a severe drop in the intracellular ATP levels, caused either by uncompensated loss to the medium, unchecked hydrolysis of the cellular ATP, or an inhibition of ATP production via glycolysis. The results described here have shown that the ATP level within the cells remains at the preinfection level under conditions where one sees the two-step fluorescence increase; this eliminates the first and second of the possible explanations. Also, the sum of the intracellular and extracellular ATP levels increases substantially over at least 36 min; this eliminates the third possibility. It seems that a principal, remaining hypothesis is that the net membrane-energizing effectiveness or the hydrolytic activity of the membrane-bound ATPase is disturbed.

To determine whether a drop in the intracellular ATP level could have been detected under our conditions, we treated cells with colicin K and we did observe a decrease to about three-fourths the preinfection level (data not shown), consistent with the results of Plate et al [30]. T5 infection caused total ATP (combined intracellular and extracellular) to increase, indicating that the cells were still able to produce ATP via glycolysis. We believe our determinations of extracellular ATP to be reliable, also. If lysis were a significant factor, we would expect to see a decrease in extractable ATP from cell pellet; expressed on a per cell basis, the rise in extracellular ATP is too large to be due solely to this cause in any case. Colicins E1 and K, which disrupt energy metabolism, cause total ATP to rise within cells with disabled membrane-bound ATPase [31].

The increase in extracellular ATP tails off at about 2.5×10^6 molecules ATP per cell; on the basis of constants from Materials and Methods, this is approximately 34 μ M in the medium. Using the literature value for cell water volume, approximately 2.4 μ l/mg cell dry wt [32–35], intracellular ATP concentration is calculated as 1.6 mM. The discrepancy suggests that 1) little intracellular ATP is in equilibrium with medium; 2) ATP production

exceeds loss to medium; 3) the intracellular ATP level is maintained and regulated, and release at later times is hindered; or 4) a combination of these factors. We have no quantitative explanation for the observed ATP levels.

ATP excretion seems part of a more general phenomenon; T5 degrades host DNA starting within 3 min after infection, and the breakdown products are found in the medium [36].

Uncoupling and change of membrane permeability are not "all or none" phenomena. The observed increase of ANS-fluorescence under anaerobic conditions induced by T5 could be explained by a more general membrane damage. The ATP-dependent proton pump may simply be too weak to maintain a proton-motive force across the leaky membrane that can be measured by ANS-fluorescence. In contrast, due to its high capacity, the respiration-dependent pump can build up a proton-motive force, which can be seen by ANS-fluorescence quenching.

Other laboratories have investigated the usefulness of ANS fluorescence as an indicator of the energetic state of whole *E. coli* cells [4, 5, 22] and have concluded that the probe reports on a high-energy state that can be generated by O_2 -dependent respiration, or more generally by a CCCP-sensitive process or processes. Our experience with ANS strongly suggests that it responds to changes in more than just one cell condition. With cell concentrations up to about 10^{10} cells per milliliter, there is a moderately large increase in fluorescence as, for example the cells use up the last of the available fermentable energy source anaerobically; this increase can be reversed by addition of an electron acceptor for at least an hour, or it can be reversed by addition of a fermentable substrate. At even higher cell densities anaerobic, fermenting cells acidify their medium (data not shown) and cause ANS fluorescence to rise very strongly. This rise is aeration-reversible to a great extent but is of course not reversible by the addition of a fermentable substrate. This kind of ANS fluorescence rise has been avoided and does not concern us here. A third kind of fluorescence rise is that seen immediately after T5 infection (step 1-like), which is reversible neither by aeration nor by a fermentable substrate and which, as we have mentioned above, is correlated with a permeability breakdown. The magnitude of this rise is related to the severity of the damage to the permeability barrier. In view of these findings, it seems that some of the literature concerning cell-ANS fluorescence may actually deal with a combination of effects that in the T5 system are time-resolved into two or more distinct responses. Since we have observed ANS and NPN to behave similarly under all conditions tested, these comments probably apply also to systems using NPN in work with phages [6, 7], colicins, and a variety of metabolic inhibitors and uncouplers [21, 37, 38].

ACKNOWLEDGMENTS

The authors thank Carola Scherer, of this institute, for providing data on ATP levels during phage infection. We also wish to extend our sincere thanks to Dr. Benno Hess for making available the facilities of the Max-Planck-Institut für Ernährungsphysiologie in Dortmund, where we performed experiments that allowed us to interpret the fluorescence data obtained with our equipment in Tübingen and to Dr. Hans-Ulrich Schairer of the Max-Planck-Institut in Tübingen for his generous donations of bacterial strains. The research was supported by the Deutsche Forschungsgemeinschaft (SFB 76), to whom we would also like to express our appreciation.

REFERENCES

1. Braun V, Hantke K: *Ann Rev Biochem* 43:89–121, 1974.
2. Braun V, Hantke K: In Reissig JL (ed): "Microbial Interactions, Receptors and Recognition." London: Chapman and Hall, 1977, Series B, vol 3, pp 101–137.
3. Braun V: In Stanier RY, Rogers HJ, Ward BJ (eds): "Relations Between Structure and Function in the Prokaryotic Cell." Symposium XXVIII of the Society for General Microbiology. Cambridge, England: Cambridge University Press, 1978, pp 111–138.
4. Griniuvienė B, Dzheia P, Grinius L: *Biochem Biophys Res Commun* 64:790–796, 1975.
5. Reeves JP, Lombardi FJ, Kaback HR: *J Biol Chem* 247:6204–6211, 1972.
6. Hantke K, Braun V: *Virology* 58:310–312, 1974.
7. Braun V: *Zentralbl Bakteriol, Parasitenkd, Infektionskr Hyg Abt 1 Orig* 228:233–240, 1977.
8. Lanni YT: *Bacteriol Rev* 32:227–242, 1968.
9. Lanni YT: *Proc Natl Acad Sci USA* 53:969–973, 1965.
10. McCorquodale DJ, Buchanan JM: *J Biol Chem* 243:2550–2559, 1968.
11. Clowes RC, Hayes W (eds): "Experiments in Microbial Genetics." Oxford: Blackwell Scientific Publications, 1968, p 187.
12. Tanaka S, Lerner SA, Lin ECC: *J Bacteriol* 93:642–648, 1967.
13. Cohen GN, Rickenberg HW: *Ann Inst Pasteur, Paris* 91:693, 1956.
14. Anraku Y: *J Biol Chem* 242:793–800, 1967.
15. Lester RL, DeMoss JA: *J Bacteriol* 105:1006–1014, 1971.
16. Yamamoto KR, Alberts BM, Benzinger R, Lawhorne L, Treiber G: *Virology* 40:734–744, 1970.
17. Zweig M, Cummings DJ: *Virology* 51:443–453, 1973.
18. Estabrook RW, Williamson JR, Frenkel R, Maitra PK: *Methods Enzymol* 10:474–482, 1967.
19. Schairer HU, Gruber D: *Eur J Biochem* 37:282–286, 1973.
20. Mathis RR, Brown OR: *Biochim Biophys Acta* 440:723–732, 1976.
21. Cramer WA, Postma PW, Helgerson SL: *Biochim Biophys Acta* 449:401–411, 1976.
22. Griniuvienė B, Chmieliauskaitė V, Melvydas V, Dzheia P, Grinius L: *J Bioenergetics* 7:17–37, 1975.
23. Haynes DH: *J Membrane Biol* 17:341–366, 1974.
24. Pudek MR, Bragg PD: *Arch Biochem Biophys* 164:682–693, 1974.
25. Pudek MR, Bragg PD: *FEBS Lett* 50:111–113, 1975.
26. Harold FM, Baarda JR, Baron C, Abrams A: *J Biol Chem* 244:2261–2268, 1969.
27. Altendorf K-H, Harold FM: *J Biol Chem* 249:4587–4593, 1974.
28. Fillingame RH: *J Bacteriol* 124:870–883, 1975.
29. Oldmixon F, Braun V: *Biochim Biophys Acta* 506:111–118, 1978.
30. Plate CA, Suit JL, Jetten AM, Luria SE: *J Biol Chem* 249:6138–6143, 1974.
31. Feingold DS: *J Membrane Biol* 3:372–386, 1970.
32. Mitchell P, Moyle J: *Symp Soc Gen Microbiol* 6:150–180, 1956.
33. Kashket ER, Wong PTS: *Biochim Biophys Acta* 193:212–214, 1969.
34. Alemohammad MM, Knowles CF: *J Gen Microbiol* 82:125–142, 1974.
35. Cook AM, Urban E, Schlegel HG: *Analyt Biochem* 72:191–201, 1976.
36. Warner HR, Drong RF, Berget SM: *J Virol* 15:273–280, 1975.
37. Nieva-Gomez D, Konisky J, Gennis RB: *Biochemistry* 15:2747–2753, 1976.
38. Brewer GF: *Biochemistry* 13:5038–5045, 1974.